

Available online at www.sciencedirect.com

Procedia Computer Science 4 (2011) 811–820

Procedia
Computer Science

Pulsatile flow in model cerebral aneurysms

Julia Mikhal^{a,*}, Bernard J. Geurts^{a,b}^a*Multiscale Modeling and Simulation, Dept. of Applied Mathematics, University of Twente, P.O. Box 217, 7500 AE Enschede, The Netherlands*^b*Anisotropic Turbulence, Dept. of Applied Physics, Eindhoven University of Technology, P.O. Box 513, 5600 MB Eindhoven, The Netherlands*

Abstract

We present an immersed boundary method based on volume penalization, with which pulsatile flow in a model cerebral aneurysm is simulated. The model aneurysm consists of a curved vessel merged with a spherical cavity. The dominant vortical structures arising in the time-dependent flow are discussed and the evolution of the maximal shear stress in the aneurysm is analyzed. We approximate flow properties of blood by those of an incompressible Newtonian fluid. The flow inside the aneurysm is simulated with the use of a skew-symmetric finite-volume discretization and explicit time-stepping. We focus on effects due to variations in the amplitude of the pulsatile flow as well as due to changes in the Reynolds number (Re) by studying flow at $Re = 100$, 250 and 500. At $Re = 500$ a complex time-dependence in the shear stress levels is observed, reflecting the lively development of the flow in the model aneurysm in which vortices are created continuously inside the curved vessel and in the spherical cavity of the aneurysm. An increase in the amplitude of the pulsatile flow increases the shear stress levels somewhat, but at $Re = 500$ the flow is mainly dominated by its intrinsic unsteadiness. Reducing the Reynolds number yields a stronger contribution of the periodic pulsatile flow forcing: at $Re = 100$ we find a strong dominance of shear stress levels due to the forcing, while at $Re = 250$ the intrinsic and pulsatile unsteadiness are of comparable importance.

Keywords:

cerebral aneurysm, pulsatile flow, immersed boundary method, volume-penalization, incompressible flow, shear stress

1. Introduction

There is a growing medical need to obtain predictions of the flow behavior and shear stresses inside the human brain that is specific to individual patients. The prediction of the flow constitutes a challenging and timely computational multiscale modeling problem, aimed at understanding and identifying the likelihood of long-time rupture from an analysis of short-time pulsatile flow [13]. Understanding such pulsatile flow patterns will help to describe long-time accumulation effects such as the growth of an aneurysm, or the deterioration of the vessel wall due to reduced blood circulation. This capability allows also a more complete planning of surgical intervention and can be used to predict the effectiveness of such procedures. A huge amount of work has been done on Computational Fluid Dynamics (CFD) of flow in the human brain and in the cardiovascular system [11, 2, 1, 12, 6, 3]. The most commonly adopted numerical approach is the finite element method. This method can, in principle, represent highly complex geometries but at considerable expense, particularly when dealing with raw biomedical imagery to define vessel geometries

*Corresponding author.

Email address: j.mikhal@ewi.utwente.nl (Julia Mikhal)

2. Numerical method

In this section we introduce the fluid-mechanical model that is used to simulate blood flow in cerebral aneurysms. The numerical method employs a volume-penalization immersed boundary (IB) method, which is briefly reviewed and illustrated for the geometry of a curved blood vessel. For viscous flow at Reynolds number $Re = 1$ we present convergence findings achieved by grid refinement.

There is a number of different approaches to model flow of blood in the human brain. A comprehensive overview is given in [12]. One way is to approximate blood as a simple Newtonian fluid with constant viscosity [2]. More refined models include the shear-thinning behavior of blood by adopting, e.g., the Carreau-Yasuda model to capture non-Newtonian rheology [1, 6]. Under physiological flow conditions in sufficiently large arteries the non-Newtonian corrections were found to be quite small [11, 3]. The main flow features were the same as in Newtonian flow, albeit at somewhat different stress and velocity levels. In this paper we study to what extent an immersed boundary method is suitable to simulate time-dependent flow in the circle of Willis; for these low Reynolds flows in larger cerebral vessels non-Newtonian corrections are neglected. Hence, we restrict to incompressible Newtonian fluid mechanics as represented by the Navier-Stokes equations. The total physical domain Ω consists of a fluid part Ω_f and a complementary solid part Ω_s . The interface between the two will be identified as $\partial\Omega_f$ at which the no-slip condition applies. The governing equations, completed with a no-slip boundary condition on the solid walls of the domain are given in non-dimensional form by:

$$\frac{\partial \mathbf{u}}{\partial t} + \mathbf{u} \cdot \nabla \mathbf{u} = -\nabla p + \frac{1}{Re} \nabla^2 \mathbf{u} + \mathbf{f} \quad (1)$$

$$\nabla \cdot \mathbf{u} = 0 \quad (2)$$

$$\text{with } \mathbf{u} = \mathbf{0} \text{ at } \partial\Omega_f \quad (3)$$

where \mathbf{u} is the velocity of the fluid in the domain Ω , p is the pressure and $Re = UL/\nu$ is the Reynolds number, in terms of a reference velocity U , a reference length scale L and the kinematic viscosity $\nu = \mu/\rho$ with molecular viscosity given by μ and the fluid mass density ρ . In our model the length scale is of the order of the diameter of a vessel connecting to an aneurysm cavity, while the reference velocity is of the order of the bulk velocity derived from the mass flow-rate Q and the cross-sectional area of a vessel A , i.e., $U = Q/A$. Obviously, the velocity inside the solid regions should vanish. This may be expressed to very close approximation by a proper selection of the forcing term \mathbf{f} giving rise to a volume penalization immersed boundary method [10]. We describe this approach in more detail next.

The IB method provides an alternative to conventional numerical simulation methods in case flow in and around very complex spatial domains is considered. Conventional methods adhere to computational meshes that are body-fitted. With this approach the gridding of the fluid region becomes very time consuming for complex domains. The task of generating grids that yield an accurate discrete computational model is correspondingly difficult, up to the point of becoming impractical. Instead, the IB method can be formulated entirely in terms of an uniform Cartesian grid. The geometry over and through which the flow takes place is simply immersed in a ‘block’ of physical space. These striking differences in the computational strategies also imply important consequences for the accuracy with which flow near solid boundaries may generally be captured. Conventional body-fitted methods allow, in principle, for a precise representation of no-slip conditions at the body. In contrast, the accuracy achieved by an IB method generally is reduced by the fact that the geometry is not aligned with the Cartesian grid and the location of the solid-fluid interface is known only to within a grid-spacing. The accuracy of the resulting IB method will be considered for the velocity field \mathbf{u} as well as its gradient, e.g., in terms of the shear stresses that develop. As illustrated in [8] reliable results can readily be obtained at moderate Reynolds numbers, even with the coarse staircase approach to the solid-fluid interface.

The forcing term \mathbf{f} in our IB method represents the impenetrability of a stationary solid wall to fluid flow. It is approximated by direct penalization of the flow from entering the solid domain by choosing

$$\mathbf{f} = -\frac{1}{\varepsilon} H(\mathbf{x}) \mathbf{u}(\mathbf{x}, t) \quad (4)$$

The control parameter $\varepsilon \ll 1$ (a typical value used here is $\varepsilon = 10^{-10}$) and $H(\mathbf{x})$ is the so-called ‘masking function’ which distinguishes fluid parts from solid parts of the computational domain. For a point \mathbf{x} which belongs to a fluid

[2, 6, 3]. As an alternative approach, designed primarily to treat flow in domains of realistic complexity, we present the development and application of an immersed boundary (IB) method capable to reliably compute flow and shear stresses at various flow conditions and vessel geometries. We concentrate on a generic model aneurysm with which the flow and forces are studied at a range of physiologically relevant Reynolds numbers and various amplitudes of the pulsatile flow. The effects of the pulsatile flow are found to be strongest for very viscous flow, i.e., at relatively low Reynolds numbers, while the intrinsic unsteadiness of the flow at higher Reynolds numbers is dominant.

In medical applications the shape of cerebral aneurysms developing in patients can be inferred by using three-dimensional rotational angiography [4]. In this procedure a small volume of brain tissue can be scanned, allowing an approximate identification of the fluid and the solid parts. A volume-penalization immersed boundary (IB) method is applied to represent the aneurysm geometry. In this IB approach the flow domain is characterized by a so-called ‘masking function’, which takes the value ‘0’ in a fluid part and ‘1’ in solid parts of the domain. The raw angiography data allows for a simple ‘staircase approximation’ of the vessel and aneurysm shape in which individual pixels in the digital data form the smallest unit of localization of the solid-fluid interface. This raw information specifies the masking function. We will adopt the ‘staircase’ geometry representation in this paper and do not incorporate any additional smoothing of the geometry or the use of sophisticated reconstruction methods. For a more complete modeling of the dynamics in the vessel system, flow-structure interaction often plays a role [12]. In that case also parameters and models that characterize mechanical elasticity of brain tissue are required. In this paper we restrict to developing the IB approach for relatively small cerebral aneurysms for which movements of the vessel wall is often not a primary concern and, hence, a detailed mechanical characterization is not required.

Cerebral aneurysms are most often located in the Circle of Willis – the central vessel network for the supply of blood to the human brain. The common risk-areas are at ‘T’ and ‘Y’-shaped junctions in the vessels of the Circle of Willis [5]. This motivates to analyze the flow in basic vessel and aneurysm structures by modeling them as curved cylindrical tubes to which spherical cavities are attached. The computational model for the simulation of blood flow through the larger vessels in the human brain is based on the incompressible Navier-Stokes equations. The flow inside the vessels is simulated with a skew-symmetric finite-volume discretization on a uniform Cartesian grid and explicit time-stepping. In this paper we illustrate our IB approach by predicting unsteady flow in basic cylindrical and spherical geometries. This allows a detailed assessment of the quality of the flow predictions and forms essential stepping stone problems on the way toward adopting the IB flow solver on a patient-specific basis.

The quality of the predictions depends strongly on the spatial resolution that can be afforded. From a previous study of Poiseuille flow in channels and pipes [9, 8] we inferred that about 16 grid points per coordinate direction suffice to obtain reliable laminar flow predictions. For general geometries that are not aligned with the underlying Cartesian grid, first order convergence upon grid-refinement was established. Using an energy-conserving skew-symmetric discretization [14] the IB approach was found to provide reliable information about the flow structure and associated stress levels. Such computational modeling augments current clinical data and can, in future, help improve the planning and execution of surgical interventions.

In [8] several strategies to generate a masking function were compared. For the test-case of Poiseuille flow, the analysis of the numerical method showed an overall first order convergence. This low convergence order is associated with the non-alignment of the geometry with the underlying Cartesian grid. Flow emerging from steady forcing was investigated and the laminar velocity and shear stress distribution were computed. In this paper we focus on pulsatile flow through a model aneurysm, i.e., we investigate the flow response to a time-dependent, prescribed mass flow rate. For convenience we impose a sinusoidal function for variations in the mass flow rate and investigate effects arising from changes in the pulsatile amplitude at various Reynolds numbers, taken in the range 100-500 to comply with clinical data in [7, 12]. The IB method in combination with skew-symmetric finite volume discretization was found suitable to capture the dominant flow structures and the corresponding time-dependent shear stresses on the aneurysm walls. At sufficiently low Reynolds number, e.g., at sufficiently low fluid velocity or at sufficiently high viscosity, the effect of periodic variation in the mass flow rate dominates the developing flow. Conversely, at higher Reynolds numbers the flow displays an intrinsic unsteadiness associated with the nonlinearity in the Navier-Stokes equations, which is strong enough to overwhelm the detailed periodic variations in the flow rate.

The organization of this paper is as follows. In Section 2 we present a brief sketch of the IB method that is applied to the curved vessel geometry and discuss the convergence of numerical predictions. The dynamics of pulsatile flow is discussed in Section 3 and an analysis of shear stress levels in pulsatile flow is given in Section 4. Concluding remarks are in Section 5.

part Ω_f the masking function $H(\mathbf{x}) = 0$. Correspondingly, around such a location the regular Navier-Stokes system in (1)-(2) is employed. For any location inside the solid part Ω_s of the domain the masking function H takes the value 1. Since ε is chosen very small, the forcing inside the solid domain dominates all other fluxes in the Navier-Stokes equations.

The form of the forcing \mathbf{f} inside the solid part implies that the velocity component \mathbf{u} is negligible; if at some location in the solid \mathbf{u} would, for some reason, have become non-zero then the forcing drives the local velocity exponentially quickly back to negligible values. In the region near the interface between the solid and the fluid parts of the domain the velocity field would be forced to negligible values within a very thin strip of the grid. A sufficiently small value of ε will imply a very localized region in which a non-trivial flow in Ω_f connects to a solution with negligible values in Ω_s . This rough sketch identifies that the simple volume forcing (4) can indeed approximate a no-slip boundary condition, localized to within one grid cell. Thus, accurate results can in principle be achieved provided the spatial resolution is adequate.

Numerically the equations resulting from the introduction of the forcing (4) in the Navier-Stokes equations are treated with a finite-volume discretization where the skew-symmetry of the nonlinear convective fluxes and the positive-definite dissipative nature of the viscous fluxes are preserved [14]. This method can be shown to be stable on any (coarse) resolution, with a proper treating of a small scale details in a numerical solution. In order to capture forces on the solid walls of the domain the treatment of the small near-wall flow structures is essential. A second order accurate method for the fluxes is employed, implemented on a staggered grid. The effect of these fluxes is integrated in time using an explicit time-stepping algorithm of Adams-Bashforth type [14]. The contribution of the forcing term \mathbf{f} is integrated implicitly in time, which overcomes severe stability problems that would arise with explicit methods as $\varepsilon \ll 1$. The total computational domain is endowed with periodic boundary conditions. In order to generate a non-trivial flow we impose a time-dependent pressure drop across the streamwise direction x , chosen such that the desired unsteady flow-rate is maintained. In total, the pressure can be expressed at $a(t)x + p$ where $p(\mathbf{x}, t)$ denotes a periodic pressure field and $a(t)$ is the time-dependent pressure gradient across the domain in the x direction.

The use of a staggered grid introduces the question how to define exactly the masking function. Intuitively, H is easily defined as indicated above. However, there is some freedom in its definition on grid-scale near a solid-fluid interface. We work with an individual grid cell as the smallest elementary unit; this implies that a grid cell is considered either as part of the solid or as part of the fluid. We need to identify on which component of the solution to base the masking function as all three velocity components u, v, w and the pressure p are defined on their respective grids. We choose to work with H_p , which means that if the center of a primary grid cell is in the fluid domain, then the entire grid cell is defined as part of Ω_f . This allows to define the precise location (within the resolution of the adopted grid) of the solid-fluid interface in a ‘staircase’ approximation. The convergence of the volume-penalization IB method can be established on the basis of laminar Poiseuille flow in a straight cylindrical tube. This test-case was considered in [8] and first-order convergence was observed. This confirms results obtained for the plane channel flow in case the no-slip condition is imposed within a grid cell of the solid wall [9].

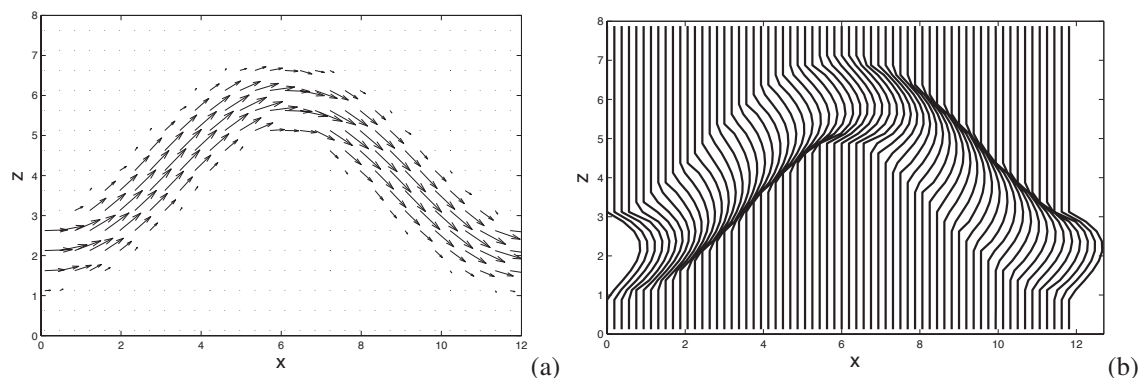


Figure 1: Application of the immersed boundary method to flow in a curved cylindrical vessel. Simulations are done for laminar flow at $Re = 1$. The flow is visualized by plotting velocity vectors (a) and velocity profiles of the streamwise velocity component (b) in a cross-section through the geometry at grid resolution $64 \times 16 \times 32$.

The geometry of blood vessels in a human brain is much more complicated than straight cylindrical tube. The first step towards simulating flow in more realistic vessel shapes is to consider smoothly curved geometries. To obtain the masking function for such a vessel we rely on the smallest distance of a point \mathbf{x} to the centerline of the curved vessel. For each point of the computational domain we can find the minimal distance to this centerline and check the condition whether or not this distance is smaller than the radius of the cylindrical tube. If so, then the point (grid cell) is in the fluid domain and the masking function $H = 0$. Otherwise it is in solid domain and $H = 1$.

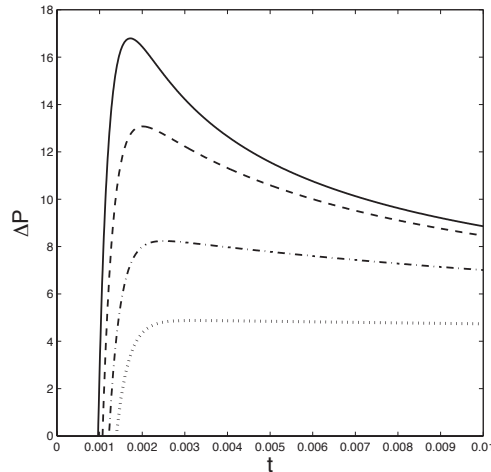


Figure 2: The convergence of the immersed boundary method for the flow inside a curved cylindrical vessel is shown in terms of the evolution of the pressure difference. Simulations are done for laminar flow at $Re = 1$ at several grid resolutions: $32 \times 8 \times 16$ (dot), $64 \times 16 \times 32$ (dash-dot), $128 \times 32 \times 64$ (dash) and $256 \times 64 \times 128$ (solid). With increasing grid resolution the numerically obtained solution is seen to converge.

To illustrate the IB method for curved vessels we consider simple sinusoidal shapes for the centerline and a constant circular cross-section in a plane locally normal to the tangent vector to the centerline. Simulations at $Re = 1$ as shown in Figure 1(a) clarify that the steady flow which develops closely follows the shape of the vessel. At each location a well-defined velocity profile emerges as is seen in Figure 1(b). To illustrate the convergence of the method for curved vessel we consider the pressure difference over the flow domain in the x -direction. The development of this pressure difference at a number of spatial resolutions is displayed in Figure 2. We observe a clear convergence in these pressure evolutions by comparing results obtained at $N = 32, 64, 128$ and 256 . For longer simulation time all these solutions converge to a steady state.

3. Reference pulsatile flow dynamics

In this section we consider the dynamics of pulsatile flow in a model aneurysm. First, we define the geometry of the model aneurysm and motivate the adopted flow conditions. Subsequently, we analyze the velocity field and shear forces for the reference case and compare the main characteristics as pressure drop and maximal shear stress for pulsatile and constant mass flow rate which have the same average flow.

One of the common locations of cerebral aneurysms within the Circle of Willis is on the internal carotid artery (ICA), where a typical mass flow rate is reported to be $Q \approx 245 \text{ ml/min}$ [5]. The diameter of the ICA is of the order of $D \approx 0.42 \text{ cm}$ [7]. Together, this leads to a reference velocity $U \approx 0.2947 \text{ m/s}$ and a corresponding Reynolds number $Re \approx 354$ in which we used as reference kinematic viscosity $\nu = 3.5 \cdot 10^{-6} \text{ m}^2/\text{s}$ [12]. The natural variation in conditions and geometry motivate to use Reynolds numbers in the general range of 100-500, properly including this estimate obtained from literature.

The Reynolds number Re is the only parameter which is required to specify the flow conditions. It quantifies the ratio between the magnitude of the (destabilizing) convective transport $\mathbf{u} \cdot \nabla \mathbf{u}$ and the (stabilizing) viscous processes $\nabla^2 \mathbf{u}$. It is well known that for relatively small Reynolds numbers flow is laminar and steady, which implies a smooth

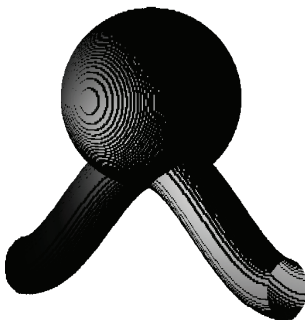


Figure 3: Three dimensional geometry of the model aneurysm that is constructed of a curved vessel and a spherical cavity attached to it.

velocity and pressure field at every moment in time. With increasing Reynolds number the flow can develop more detailed vortical structures, e.g., associated with separated flow near relatively abrupt changes in the shape of a vessel. A further increase in Re usually implies that the flow structures become unsteady with different vortices. The range of Reynolds numbers arising in the flow in the Circle of Willis, as estimated above, corresponds to laminar flow. As point of reference we chose to work with Reynolds number $Re = 500$.

The flow domain is composed of a simple sinusoidally shaped cylindrical tube of radius R to which we add a spherical cavity of radius $3R$, thus arriving at a configuration that generates significant flow separation. As reference length scale we adopt the basic radius R of the vessel. The geometry of the model aneurysm is based on a model for curved blood vessel, which was described above in Section 2. The three dimensional geometry of the model aneurysm is represented in Figure 3. The walls of the model aneurysm are assumed to be stationary in our studies reported here. Further refinements in which flow-structure interactions will be included are subject of current research.

The blood flow in a human body is pulsatile. Every person has their own complex heart beat characteristics. These depend on all sorts of parameters [12]. One cardiac cycle consists of two phases: systole and diastole. Depending on a stage the blood mass flow rate is higher or lower than average. In our investigations here we do not consider all details of a real cardiac cycle, but concentrate on a simple sinusoidal pulsatile flow, representing a Fourier component of the total cardiac pattern. We specify the average mass flow rate and add a sinusoidal perturbation for which the amplitude and the frequency can be varied. As point of reference the amplitude of the sinusoidal pulse is taken 10% of the average flow rate. The period of the oscillations is set to $T = 20$.

In Figure 4(a,b) we show the developing flow in the model aneurysm. Two snapshots of the unsteady flow are plotted. The addition of a spherical cavity is seen to strongly affect the flow in the curved vessel, which leads to massive flow separation, e.g., from the rim of the spherical cavity. This produces a detached ‘jet’ that continuously impinges on the wall of the cavity. The flow shows complex vortical structures that fill a large part of the spherical cavity with recirculating flow. The occurrence of such flow structures contributes to an extension of the average ‘residence time’ of blood inside the flow domain, expressing a deterioration of the quality of transport of nutrients to, and waste products from the tissue surrounding the aneurysm. This can be an important indicator for the rate at which health risks may develop.

The main challenge for the IB method in case of flow through model aneurysms is in capturing the flow near the solid-fluid interface, which is required to compute the shear stress. We define the shear stress in terms of the gradient of the velocity as follows. The rate of strain tensor \mathbf{S} is such that

$$S_{ij} = \frac{1}{2}(\partial_i u_j + \partial_j u_i) \quad (5)$$

The shear stress τ is a measure of the components of \mathbf{S} . It is defined as

$$\tau = \frac{1}{Re} \sqrt{2 S_{ij} S_{ij}} \quad (6)$$

The distribution of the shear stress τ is an important indicator for the forces inside the model aneurysm and on its wall. The shear stress is also relevant for long-time accumulation effects that can lead to a deterioration of the quality

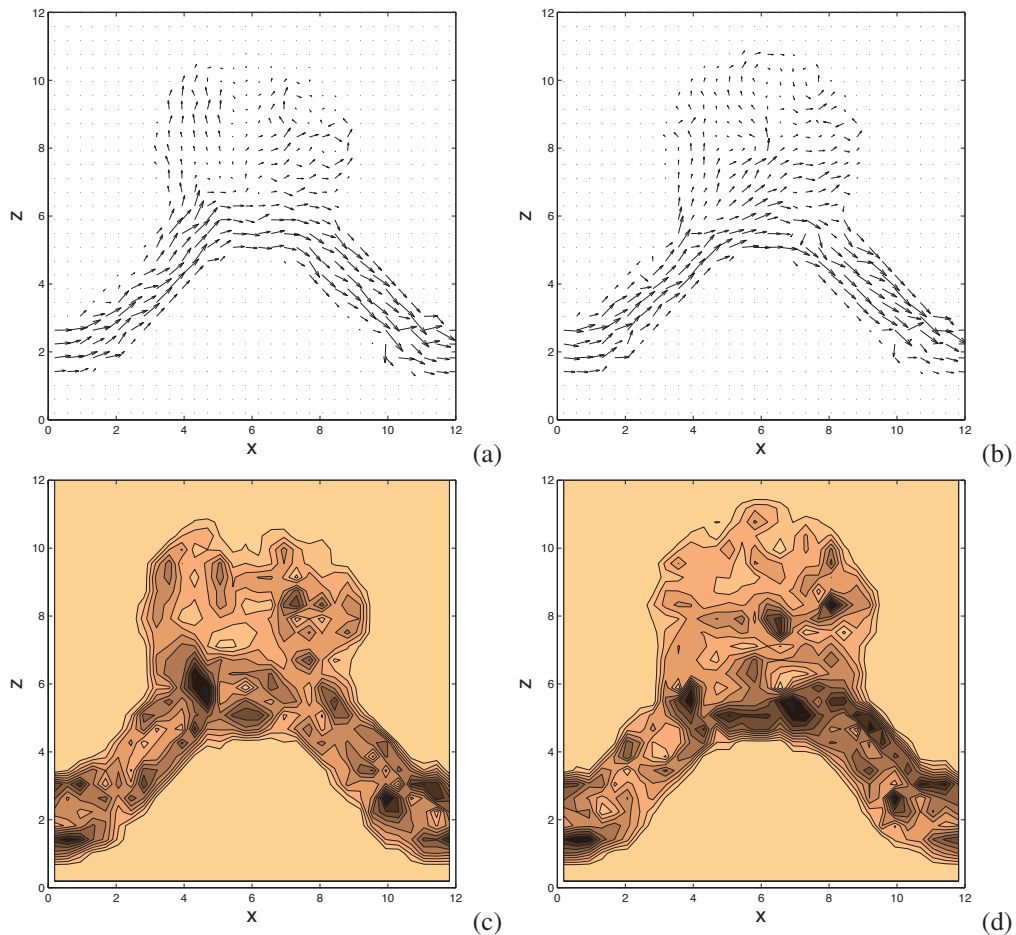


Figure 4: Velocity vector field and shear stress distribution inside the model aneurysm. Simulations are done for pulsatile flow at $Re = 500$. The period of the pulsatile flow is $T = 20$ while the amplitude is 10% of the long-time average. The flow is visualized by plotting velocity vectors in a cross-section through the geometry at grid resolution $32 \times 16 \times 32$. Two snapshots of velocity fields at time $t = 50$ (a) and time $t = 100$ (b) illustrate the unsteady flow with various vortices inside the spherical cavity. Correspondingly, in (c) and (d) the characteristic impression of the shear stress is shown. Dark regions relate to the areas with high shear stress values.

of the fluid-solid interface. This makes the shear stress a key quantity of relevance for the prediction of long-term risk of rupture of the aneurysm wall. In Figure 4(c,d) we show shear stress distributions at two characteristic moments during the evolving flow. We observe high shear stress levels in the curved vessel as well as associated with localized vortices inside the spherical cavity.

In order to better understand the impact of pulsatility we compare pressure drop and shear stress obtained at constant and pulsatile flow. In Figure 5(a) we observe a strong effect of the pulsatile flow forcing on the pressure drop across the domain. The maximal shear stress in Figure 5(b) shows a very complex time dependence with strong variations in the shear stress and occasionally very high values. The shear stress does not display a very clear signature of the periodic flow forcing at this high value of Re . At these conditions the intrinsic unsteadiness of the flow is considerably stronger than the effect of forcing. In the next section we consider the dynamics of the flow under a range of forcing and flow conditions.

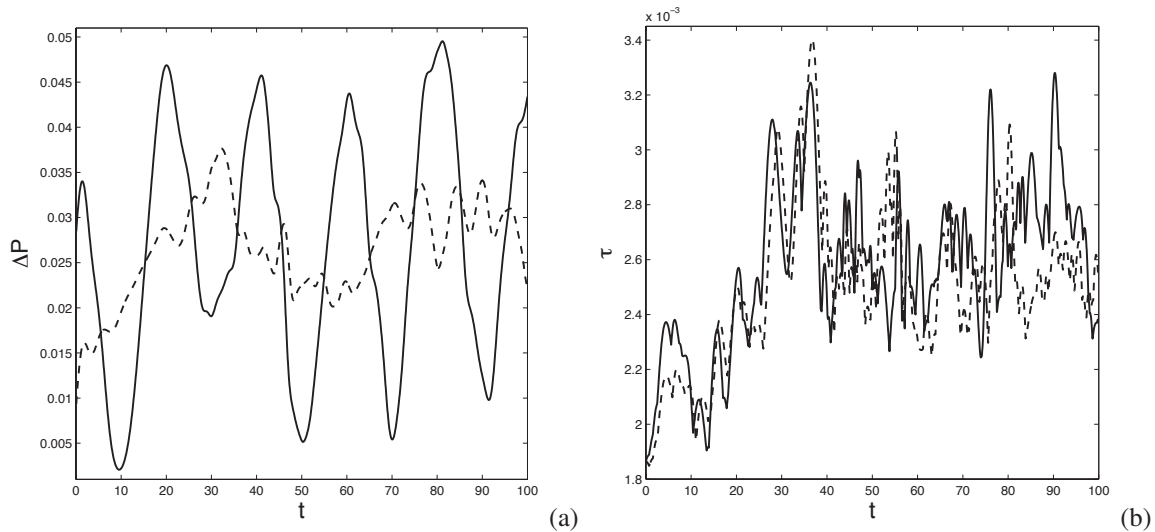


Figure 5: Pressure drop over the streamwise direction (a) and maximal shear stress in the domain (b). We compare flow with constant mass flow rate (dash) with pulsatile flow at the same average flow rate (solid). Simulations are done at $Re = 500$. The period of the pulsatile flow is $T = 20$ and the amplitude of flow rate variations is 10% of the long-time mean.

4. Pressure drop and shear stress levels in pulsatile flow

In this section we consider the effect of varying the forcing amplitude and the effect of changing the flow conditions. These illustrate the flexibility and robustness with which the IB method can handle a range of dynamic conditions.

In Figure 6 we show pressure drop and shear stress levels at $Re = 500$ and a range of amplitudes of the pulsatile variations in the flow rate. The main signature of the pressure drop and the shear stress is the same as that observed in Figure 5, the main difference being that an increase in the forcing amplitude leads to a somewhat stronger response in the shear stress. As remarked earlier, at $Re = 500$ the intrinsic dynamics of the flow at the selected mean flow rate is sufficiently strong to overwhelm the effects of the pulsatile flow as far as the shear stress is concerned.

We next present results for different Reynolds numbers, fixing the amplitude of the pulsatile oscillations to 10%. We consider $Re = 100$, 250 and 500. There are two, dynamically different situations that correspond to these variations in the Reynolds number. If (situation A) we would keep the mass flow rate unchanged then a decrease in the Reynolds number, assuming fixed geometry, corresponds to an increase in the fluid viscosity. If (situation B) at fixed geometry, we intend to keep the viscosity fixed, i.e., keep the physical properties of the fluid fixed, then a reduction in Re has to be accompanied with a reduction in the flow rate with the same factor. The two situations A and B will be presented next.

We investigated the evolution of the pressure drop and the shear stress for situation A, i.e., the fixed flow rate situation. The effect of pulsatility is stronger at lower Re , i.e., in case the fluid is more viscous. To maintain a given flow rate while increasing the viscosity, we observed that the pressure drop needs to be increased. In Figure 7(a) the shear stress levels are seen to increase with increasing viscosity. This response is in stark contrast with situation B in which we vary the Reynolds number, while keeping the viscosity of the fluid and the geometry fixed. In situation B we noticed that a reduction of the Reynolds number, i.e., a slower flow, implies a reduction in the pressure drop over the domain. The shear stress levels are seen to be lower when the Reynolds number is reduced (Figure 7(b)). Not only the level but also the complexity of the shear stress response is considerably diminished with reduced Reynolds number. All these findings correspond directly with physical intuition, illustrating the qualitative reliability of the simulations.

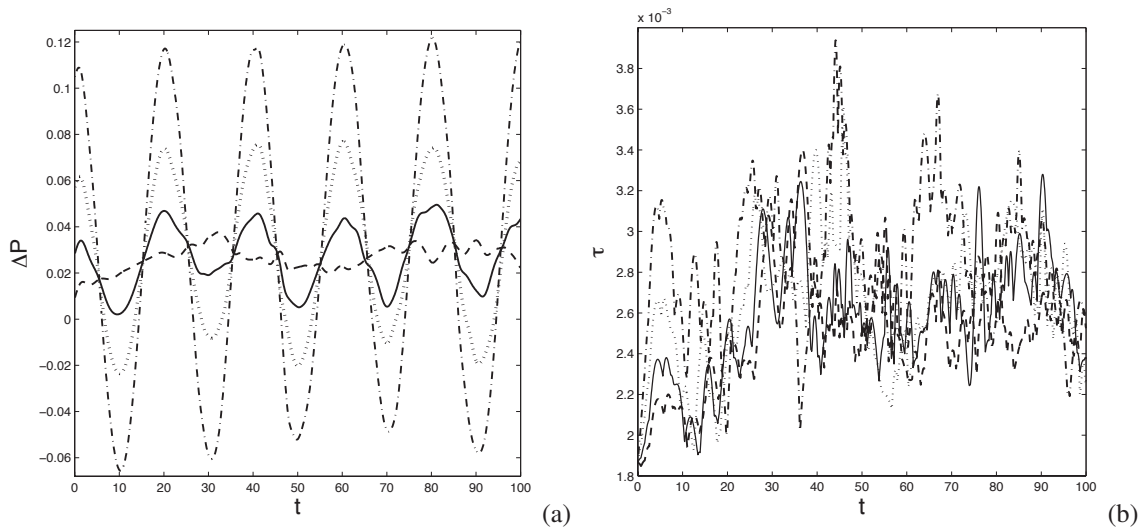


Figure 6: Pressure difference across the streamwise direction (a) and maximal shear stress (b) comparing flow with a constant mass flow rate (dash) with pulsatile flow at the same average flow rate. We employ different amplitudes of the pulsatile variations (10% – solid, 25% – dot, 50% – dash-dot). Simulations are done at $Re = 500$. The period of the pulsatile flow is $T = 20$.

5. Conclusions

In this paper we presented a basic immersed boundary method (IB) for the prediction of pulsatile viscous flow in models for cerebral aneurysms. Applications of this method to simple model geometries such as a curved vessel and a model aneurysm were presented. The flow was simulated successfully using the IB approach. Complex flow structures were observed at $Re = 500$, displaying a significant flow separation inside the spherical cavity and complex, intrinsic flow dynamics that is not very sensitive to external flow rate variations. Such would correspond to an aneurysm that developed into a considerable size in which the flow response is somewhat disconnected from the bodily rhythms. The pressure drop across the domain was found to reflect the periodic forcing much more clearly, even at high Re . The shear stress on the vessel and aneurysm walls was computed as well. At high Re a highly irregular, rapidly varying shear stress development was recorded, which could possibly induce an acceleration in the development of the aneurysm in its final stages. In order to extract more reliably such general information of clinical relevance, more research is needed into the reliability of the simulation results.

We showed the application of the IB method for a range of flow conditions and pulsatile forcing. Changes in the amplitude of the pulsatile flow do not seem to generate qualitative difference - rather an increase in the forcing amplitude leads to a corresponding increase in pressure drop and shear stress. Conversely, changes in the flow conditions can give rise to strong qualitative differences. We investigated two, physically different situations. Keeping the scale of the problem fixed we compared results at different viscosity, keeping the flow rate fixed, and results at different flow rate, keeping the viscosity fixed. The latter situation corresponds most closely to actual physiological conditions in which a higher flow rate, i.e., higher Reynolds number, requires a higher pressure drop, giving rise to higher shear stresses and considerably more complex flow development in terms of vortical structures and shear stress maxima. In case the viscosity is varied at fixed flow rate we observed the more unusual situation of an increased pressure drop and shear stress in case of a lower Reynolds number. This is solely due to the requirement of generating a fixed mass flow for an ever more viscous fluid. In each of these cases the IB method readily provided the qualitative flow consequences, even at rather coarse resolutions.

The application of computational support in the monitoring and treatment of cerebral aneurysms is a field of ongoing research. The location, time-dependence and intensity of peaks in the shear stress are all of relevance to medical practice, as these appear to be related to the long-time evolution of the condition of vessel walls. In order to achieve a closer connection with medical practice several steps need to be taken. A central element is the incorporation of realistic patient aneurysms and their coupling to proper inflow and outflow conditions. As illustrated in this paper,

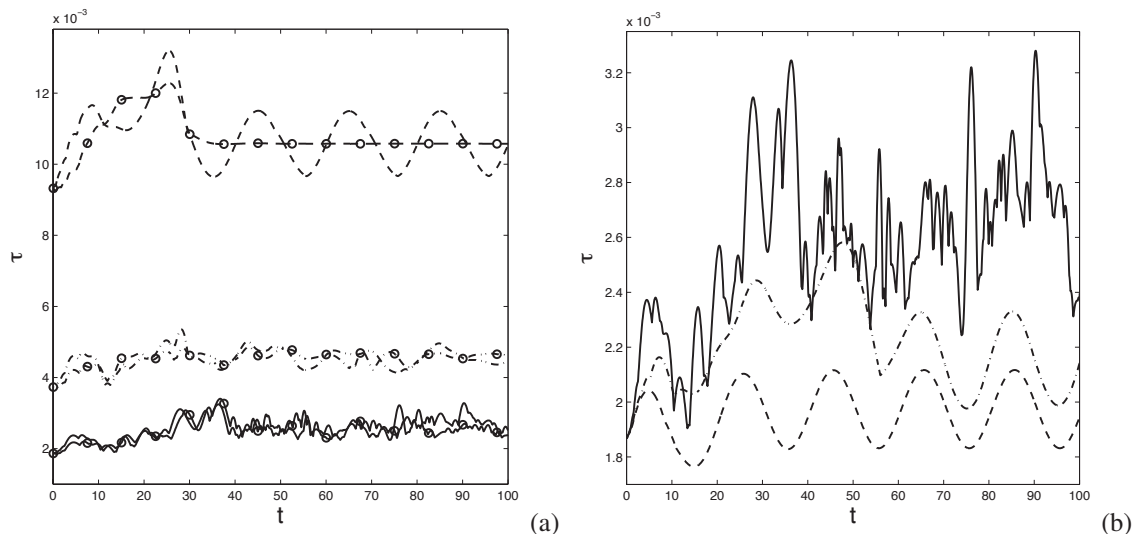


Figure 7: Maximal shear stress comparing flow with a constant mass flow rate (lines marked with circles) with pulsatile flow at the same average flow rate. The amplitude of mass flow rate variations is 10% of the long-time average. Simulations are done at $Re = 500$ (solid), $Re = 250$ (dash-dot) and $Re = 100$ (dashed) (a) changing viscosity and (b) changing flow velocity. The period of the pulsatile flow is $T = 20$.

the use of the IB method provides an invaluable point of departure for the geometric representation of complex aneurysms. The inflow and outflow conditions pose a more intricate modeling problem in which the challenge is to approximate patient-specific *in vivo* conditions. Other main elements are the inclusion of non-Newtonian fluid corrections and the proper capturing of the interaction between the flow and the aneurysm structure. In all these aspects, attention should be given to the computational robustness of predictions, focusing on the relation between the general topology of flow structures and the shear stress characteristics.

- [1] J. Bernsdorf, D. Wang, Non-Newtonian Blood Flow Simulation in Cerebral Aneurysms, *Comp. & Math. with Appl.* 58 (2009) 1024–1029.
- [2] J. R. Cebal, M. A. Castro, J. E. Burgess, R. S. Pergolizzi, M. J. Sheridan and C. M. Putman, Characterization of Cerebral Aneurysms for Assessing Risk of Rupture by Using Patient-Specific Computational Hemodynamics Models, *AJNR Am J. Neuroradiol.* 26 (2005) 2550–2559.
- [3] F. J. H. Gijssen, F. N. Van de Vosse, J. D. Janssen, The Influence of the Non-Newtonian Properties of Blood on the Flow in Large Arteries: Steady Flow in a Carotid Bifurcation Model, *Journal of Biomechanics.* 32 (1999) 601–608.
- [4] M. Grass, R. Koppe, E. Klotz, R. Proksa, M. H. Kuhn, H. Aerts, J. Op de Beek and R. Kemkers, Three-Dimensional Reconstruction of High Contrast Objects Using C-arm Image Intensifier Projection Data, *Computerized Medical Imaging and Graphics.* 23 (1999) 311–321.
- [5] J. Hendrikse, A. F. van Raamt, Y. van der Graaf, W. P. T. M. Mali and J. van der Grond, Distribution of Cerebral Blood Flow in the Circle of Willis, *Radiology.* 235 (2005) 184–189.
- [6] J. Janela, A. Moura and A. Sequeira, A 3D Non-Newtonian Fluid-Structure Interaction Model for Blood Flow in Arteries, *Journal of Computational and Applied Mathematics.* 234 (2010) 2783–2791.
- [7] S. Kamath, Observations on the Length and Diameter of Vessels Forming the Circle of Willis, *J. Anat.* 133 (1981) 419–423.
- [8] J. Mikhal, D. J. Lopez Penha, C. H. Slump and B. J. Geurts, Immersed Boundary Method Predictions of Shear Stresses for Different Flow Topologies Occurring in Cerebral Aneurysms, In proceedings of the V European Conference on Computational Fluid Dynamics, ECCOMAS CFD 2010, Lisbon, Portugal (2010).
- [9] J. Mikhal, D. J. Lopez Penha, S. Stolz and B. J. Geurts, Application of an Immersed Boundary Method to Flow in Cerebral Aneurysms and Porous Media, In proceedings of the Fluids Engineering Summer Meeting, ASME 2010, Montreal, Canada (2010).
- [10] R. Mittal and G. Iaccarino, Immersed Boundary Methods, *Annu. Rev. Fluid Mech.* 37 (2005) 239–261.
- [11] K. Perktold, R. Peter, M. Resch, Pulsatile Non-Newtonian Blood Flow Simulation Through a Bifurcation with an Aneurysm, *Biorheology* 26(6) (1989) 1011–1030.
- [12] A. Quarteroni and L. Formaggia, Mathematical Modelling and Numerical Simulation of the Cardiovascular System, *Handbook of Numerical Analysis*, Editors P.G. Ciarlet and J. L. Lions. North-Holland Vol. XII (2004) 3–127.
- [13] M. E. Sprengers, J. Schaafsma, W. J. van Rooij, M. Sluzewski, G. J. E. Rinkel, B. K. Velthuis, J. C. van Rijn and C. B. Majoie, Stability of Intracranial Aneurysms Adequately Occluded 6 Months After Coiling: A 3T MR Angiography Multicenter Long-Term Follow-Up Study, *American Journal of Neuroradiology* 29 (2008) 1768–1774.
- [14] R. W. C. P. Verstappen and A. E. P. Veldman, Symmetry-Preserving Discretization of Turbulent Flow, *J. Comput. Phys.* 187 (2003) 343–368.